NeuroImage: Clinical 4 (2014) 274–282

Contents lists available at ScienceDirect

NeuroImage: Clinical

journal homepage: www.elsevier.com/locate/ynicl

Visual and proprioceptive interaction in patients with bilateral vestibular loss ☆

Nicholas J. Cutfield [a,b], Gregory Scott [c], Adam D. Waldman [d], David J. Sharp [c,*], Adolfo M. Bronstein [b,**]

[a] Department of Medicine & Brain Health Research Centre, University of Otago & Neurology, Dunedin Hospital, Southern District Health Board, Dunedin, New Zealand
[b] Neuro-otology Unit, Division of Brain Sciences, Imperial College London, UK
[c] Computational, Cognitive and Clinical Neuroimaging Laboratory, Division of Brain Sciences, Imperial College London, UK
[d] Department of Imaging, Division of Brain Sciences, Imperial College London, UK

ARTICLE INFO

Article history:
Received 25 June 2013
Received in revised form 21 December 2013
Accepted 24 December 2013
Available online 4 January 2014

Keywords:
Functional brain imaging
Vestibular
Proprioception
Visual cortex

ABSTRACT

Following bilateral vestibular loss (BVL) patients gradually adapt to the loss of vestibular input and rely more on other sensory inputs. Here we examine changes in the way proprioceptive and visual inputs interact. We used functional magnetic resonance imaging (fMRI) to investigate visual responses in the context of varying levels of proprioceptive input in 12 BVL subjects and 15 normal controls. A novel metal-free vibrator was developed to allow vibrotactile neck proprioceptive input to be delivered in the MRI system. A high level (100 Hz) and low level (30 Hz) control stimulus was applied over the left splenius capitis; only the high frequency stimulus generates a significant proprioceptive stimulus. The neck stimulus was applied in combination with static and moving (optokinetic) visual stimuli, in a factorial fMRI experimental design. We found that high level neck proprioceptive input had more cortical effect on brain activity in the BVL patients. This included a reduction in visual motion responses during high levels of proprioceptive input and differential activation in the midline cerebellum. In early visual cortical areas, the effect of high proprioceptive input was present for both visual conditions but in lateral visual areas, including V5/MT, the effect was only seen in the context of visual motion stimulation. The finding of a cortical visuo-proprioceptive interaction in BVL patients is consistent with behavioural data indicating that, in BVL patients, neck afferents partly replace vestibular input during the CNS-mediated compensatory process. An fMRI cervico-visual interaction may thus substitute the known visuo-vestibular interaction reported in normal subject fMRI studies. The results provide evidence for a cortical mechanism of adaptation to vestibular failure, in the form of an enhanced proprioceptive influence on visual processing. The results may provide the basis for a cortical mechanism involved in proprioceptive substitution of vestibular function in BVL patients.

1. Introduction

Spatial orientation, balance and gaze stabilization involve integrating multiple sensory systems, including vestibular, visual and proprioceptive signals. How and where these complementary sensory signals are integrated and processed in the human brain is not well understood. Multisensory compensation is thought to occur in the brain after the loss of sensory afferents and to play a role in clinical recovery in vestibular disorders (Dieterich et al., 2007). Clinical recovery in vestibular disorders is variable and does not correlate well with brainstem-mediated reflexive function (Kammerlind et al., 2005). A better understanding of cortical compensatory processes (Cousins et al., 2013) should inform novel therapeutic strategies.

Functional MRI studies have provided evidence for interactions between the visual and vestibular systems (Brandt et al., 1998; Dieterich et al., 2003a, 2007; Kleinschmidt et al., 2002). Visual stimulation has been shown to simultaneously activate visual cortical regions whilst deactivating vestibular cortical regions such as the parieto-insular vestibular cortex in normal subjects (Brandt et al., 1998). Conversely, vestibular stimulation deactivates visual cortical areas (Bense et al., 2001; Dieterich et al., 2003a). This has been interpreted as a 'reciprocal inhibition' of visual and vestibular signals, which may allow resolution of potentially conflicting sensory inputs and contribute to the compensation process after loss of vestibular function. In one study, visual activations were enhanced in chronic BVL patients compared to controls (Dieterich et al., 2007), however subjects with unilateral vestibular failure have also been reported as showing lesser activation from visual motion stimulation (Deutschlander et al., 2008), suggesting that more complex interactions exist.

* Correspondence to: D.J. Sharp, The Computational, Cognitive and Clinical Neuroimaging Laboratory, 3rd Floor, Burlington Danes Building, The Hammersmith Hospital, Du Cane Road, London, W12 0NN, UK. Tel.: +44 2075947991 (Office), +44 2083833160 (Sec.), +44 7590250508 (Mobile); fax: +44 207 594 8921.
** Correspondence to: A.M. Bronstein, Neuro-otology, Division of Brain Sciences, Imperial College London, Charing Cross Hospital, London W6 8RF, UK. Tel.: +44 20 3313 5525.

2213-1582/$ – see front matter © 2013 The Authors. Published by Elsevier Inc. All rights reserved.
http://dx.doi.org/10.1016/j.nicl.2013.12.013

The cervical proprioceptive system also provides head position and motion signals (Magnus and De Kleijn, 1912). In addition to vestibular–ocular reflexes there are 'neck–eye' or cervico-ocular reflexes, which are greatly enhanced in primates and patients without vestibular function thus contributing to gaze stability (Bronstein and Hood, 1986; Dichgans et al., 1973; Gdowski et al., 2001; Gresty et al., 1977; Kasai and Zee, 1978). Neck muscle vibrotactile stimulation generates a proprioceptive signal of relative head-to-trunk body position, which can induce illusions of head tilt, head rotation, visual motion and impaired pointing to visual targets (Biguer et al., 1988; Bove et al., 2002; Popov et al., 1999). The frequency of stimulus providing a proprioceptive signal required to activate the spindle afferents is typically 100–120 Hz, and lower frequencies are not effective (Karlberg et al., 2003). The illusions induced are more prominent in darkness in the absence of stabilizing visual input (Popov et al., 1999). Furthermore, these neck vibration/head position effects are also upregulated when vestibular function is absent (Popov et al., 1996). Although a weak, visually-suppressible nystagmus is also induced, the head orientation and motion illusions induced by neck vibration are thought to be due to a cerebral modification of spatial orientation rather than directly due to brainstem mechanisms (Biguer et al., 1988; Popov et al., 1999). Similarly, cervico-ocular responses, although "reflexes", are modulated by visuo-motor context and mental set (Bronstein and Hood, 1986, 1987); suggesting that cortical processes mediating spatial orientation are involved in the control of neck proprioceptive mechanisms. Direct evidence in humans for such a cortical role is however lacking.

Proprioceptive afferents have been shown to project to cerebral cortical areas common to vestibular networks (Akbarian et al., 1992; Guldin et al., 1992). In humans, two prior functional imaging studies have used vibratory stimulation of neck muscles in normal subjects. A PET study showed increased blood flow in somatosensory S2 and the medial insula (Bottini et al., 2001) and an fMRI study showed similar activations along with networks involving the intraparietal sulcus, motor, premotor and frontal eye fields (Fasold et al., 2008).

Given common cortical areas to vestibular and proprioceptive networks, and a reported visual–vestibular interaction, then it is plausible that proprioceptive head motion signals also interact with visual motion signals. Such a cervico-visual interaction has not been demonstrated at a cortical level in humans but may be prominent in BVL patients, given that these two remaining sensory inputs signaling head motion show ocular–motor interactions in such patients (Bronstein and Hood, 1987). Whether previously observed enhanced responses to neck vibration in vestibular lesion patients (Popov et al., 1996, 1999; Strupp et al., 1998) recruit cortical mechanisms or can just be explained by brainstem mechanisms (Sadeghi et al., 2011; Xerri et al., 1985), is not known.

Cortical compensatory processes after loss of vestibular function are likely to be important for clinical recovery. Therefore, the aim of this study is to examine with fMRI how proprioceptive cortical signals interact with visual (optokinetic) motion in a patient group who has lost peripheral vestibular function. The specific hypothesis we test is that patients with stable end organ bilateral vestibular hypofunction will have an altered interaction between proprioceptive head position and visual motion cortical signals shown with blood oxygen dependent (BOLD) fMRI signal. As a secondary aim, we also investigate whether these functional changes are accompanied by changes in brain structure. Voxel-based morphometry (VBM) was used to test whether there were group differences in grey matter density, which might accompany observed changes in the fMRI signal.

2. Materials and methods

2.1. Participants

Twelve subjects with absent vestibular function were recruited (6 female), mean age 51, range 29–67 years. Bilateral loss of vestibular function was established for more than 9 months in all cases, and determined by absent clinical vestibular reflexes (head impulse test and ocular counter-rolling) and by reduction of caloric and rotational responses to values <10% of the normal response, as in our previously published clinical series (Rinne et al., 1998). In addition, 8/12 patients had utricular responses recorded and found to be below the normal range as measured with the unilateral utricular centrifugation test at 400°/s (Neurokinetic Inc; USA) (Wuyts et al., 2003). All BVL patients had hearing thresholds measured by pure tone audiometry, with hearing within normal limits for age in all subjects. The cause of bilateral vestibular failure was aminoglycoside exposure (6) and idiopathic vestibular failure (6) (Rinne et al., 1998; Zingler et al., 2008). Fifteen control subjects with no vestibular or neurological deficits had a mean age of 46 (range 25–72) years, 3 female). One control subject was excluded after an incidental posterior fossa arachnoid cyst was found on structural MRI. All subjects were fully right handed, as measured by the Edinburgh Handedness Inventory. Written informed consent was obtained and the Hammersmith Hospitals NHS Trust Ethics Committee approved the study.

2.2. Data acquisition MRI

MRI was acquired with a 3 Tesla Verio clinical MRI system (Siemens, Erlangen, Germany; version B17) using a 32-channel head coil. High resolution T_1 weighted structural images were acquired volumetrically using an inversion-recovery prepared spoiled gradient echo sequence (SPGR; MPRAGE; TE 2.48 ms, TR 1560 ms, TI 900 ms, flip angle 90°; 1 mm isotropic resolution). Functional imaging was performed using a 2D echoplanar imaging (EPI) acquired blood oxygen dependent BOLD sequence (TE 30 ms, TR 2000 ms, slice thickness 5 mm, acceleration factor 2, voxel size 2.7 × 2.7 × 5 mm). Structural and EPI images were reviewed visually to exclude incidental pathology or other structural anomalies that might confound quantitative analysis.

2.3. Experimental design

The visual stimuli (motion 'M' and static 'S') were applied in a factorial design with the proprioceptive stimuli (high 100 Hz 'H' and low 30 Hz 'L') to give four conditions: 'MH', 'SH', 'ML', 'SL' representing visual motion 100 Hz vibration, visual static 100 Hz vibration, visual motion 30 Hz vibration, visual static 30 Hz vibration respectively (Fig. 1A). To maximize task efficiency, a block design was used, with 20s blocks for each condition. One run consisted of a single block of each of the four

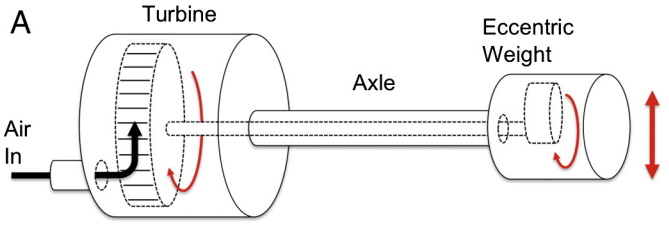

B

Proprioceptive Stimulus	Optokinetic stimulus: Motion (M)	Optokinetic stimulus: Static (S)
100Hz (H)	MH	SH
30Hz (L)	ML	SL

Fig. 1. (A): Schematic of the air turbine driven vibrotactile stimulator. The distal end is applied over the right splenius capitis. Components are Dacron and nylon. (B): The factorial design producing the four conditions visual motion/high proprioception (MH), visual motion/low proprioception (ML), static/high proprioception (SH), and static/low proprioception (SL).

conditions (80s), presented in a pseudo-randomized order. The total experiment consisted of eight runs i.e. each condition was repeated eight times. A control stimulus of a central stationary white spot on a dark background was displayed for 20s on the rear-projected LCD screen at the beginning and end of each fMRI acquisition run, during which baseline EPI images were acquired. The total duration of the factorial experiment (eight runs plus visual fixation at the beginning and end) was 11 min 20 s.

2.4. Stimuli

2.4.1. Visual motion stimulus

An angled mirror on the MRI head coil directed view to a 42-inch LCD monitor mounted 2.5 m behind the subjects' heads, giving a horizontal field of view of 21°. Vertical black and white stripes (7 black, 7 white each subtending 1.5°) were displayed in conditions static (S), and visual motion (M), tracking horizontally at 6°/s in the M condition. The direction of motion was right to left on the LCD screen, although subjects viewed this motion via the head coil mounted mirror as left to right. The visual motion paradigm and signals for airflow regulation for the vibrator were written in C/C++.

2.4.2. Neck proprioceptive stimulus

To apply a neck muscle proprioceptive stimulus which could be used during fMRI acquisition, we developed a custom Dacron and Nylon vibrotactile stimulator, driven by the air turbine rotor from a MRI limb positioning device (Elhawary et al., 2008). The turbine rotor was connected directly to an axle loaded with an eccentric Dacron 'weight', housed in a 26 mm diameter 52 mm long cylinder (Fig. 1B). The eccentric 'weight' causes the device to vibrate at a frequency determined by the incoming airflow and pressure. The device was powered by the high-pressure medical air supply, which was adjusted to the required airflow. Vibration amplitude was 0.4 mm at both high (H) and low (L) frequencies. For the fMRI experiment the vibrotactile device was applied to subjects prior to MRI acquisition for subjects to improve familiarity with the stimulus. The vibrating end of the device was firmly taped over left splenius capitis and then vacuum pads secured it into place inside the head coil. Additional vacuum-moulded pads were used to securely immobilize the head, to prevent additional head movements. We applied an identical stimulus to all subjects.

We validated the different effects of 30 Hz and 100 Hz proprioceptive stimulation conditions outside the MRI system. The vibrator was applied over the left splenius capitis of seated normal subjects in a darkened room, looking at a red LED light source. Only the 100 Hz stimulation produced illusory displacement of the light position, altered spatial and postural perception. We also verified with accelerometry that the vibration frequency was not altered by the application of the device to the subjects' necks.

In order to minimize the possibility that any fMRI findings might be due to group eye movement differences, we conducted separate ex-situ experiments in three normal subjects (ages 30–60) and one of the BVL patients, male aged 55. Subjects lied supine and were subjected to the same visual motion (OKN) and vibration protocol whilst horizontal eye movements were recorded with bi-temporal DC Electro-oculography (bandwidth 0–100 Hz, resolution 1°). Eye movements were examined and measured off-line using custom made interactive software. We found no eye movements elicited by the high or low neck vibration stimuli during the visual static condition. During the visual motion sequences a typical pattern of optokinetic nystagmus (OKN) was elicited with a mean slow phase velocity ranging from 3.5–6°/s. Applying the neck vibration stimulus did not change the underlying OKN pattern, regardless of vibration frequency. When applying the proprioceptive stimulus to BVL patients, the OKN slow phase velocity was not significantly different, ranging from 2.3 to 5.8°/s. The BVL oculographic data were indistinguishable from that of the normal subjects and within normal ranges.

2.5. Functional MRI analysis

Whole-brain fMRI data was analysed with standard random effects general linear models using tools from the FSL library (FMRIB, FEAT version 5.98) (Smith et al., 2004). Image pre-processing involved re-alignment of EPI images, spatial smoothing using a 6 mm full-width half-maximum Gaussian kernel, pre-whitening using FILM and temporal high-pass filtering using a cut-off frequency of 1/50 Hz to correct for baseline drifts in the signal. FMRIB's Linear Image Registration Tool was used to register EPI functional datasets into standard MNI space using the participant's individual high-resolution anatomical images. FMRI data were analysed using voxel-wise time series analysis within the framework of the General Linear Model (GLM). To this end a design matrix was generated with a synthetic hemodynamic response function and its first temporal derivative. Blocks from the four conditions (MH, SH, ML, SL) were modelled in the design matrix for each run.

A factorial analysis of variance (ANOVA) investigated effects of visual motion, proprioceptive input and group effects using (FMRIB's Local Analysis of Mixed Effects) (Beckmann et al., 2003). Final statistical images were thresholded using Gaussian Random Field based cluster inference with a height threshold of $Z > 2.3$ and a cluster significance threshold of $p < 0.05$.

2.6. Voxel based morphometry analysis

To test for group differences in grey matter volume, we also conducted a voxel based morphometry (VBM) analysis. Structural data was analysed with FSL–VBM, a VBM style analysis (Ashburner and Friston, 2000; Good et al., 2001) carried out using FSL tools (Smith et al., 2004). First, structural images were brain-extracted using BET (Smith, 2002). Next, tissue-type segmentation was carried out using FAST4 (Zhang et al., 2001). The resulting grey-matter partial volume images were then aligned to MNI152 standard space using the affine registration tool FLIRT (Jenkinson and Smith, 2001). Images were then averaged to create a study-specific template, to which the native grey matter images were then non-linearly re-registered. The registered partial volume images were then modulated to correct for local expansion or contraction by dividing by the Jacobian of the warp field. The modulated segmented images were smoothed with an isotropic Gaussian kernel with a sigma of 3 mm and thresholded at a nominal t value of 2.3. Finally, a voxelwise GLM was applied using permutation-based non-parametric testing, correcting for multiple comparisons across space.

3. Results

3.1. Main effect of visual motion

The main effect of motion ((MH + ML) > (SH + SL)) was associated with a similar pattern of visual cortical activation across the two subject groups (Fig. 2). As expected, peaks of activation were observed in the lingual gyrus, occipital pole bilaterally, intracalcarine cortex and the inferior part of the lateral occipital cortex bilaterally (Table 1). Bilateral activation was present in the region of V5/MT (Malikovic et al., 2007). Direct comparison of the two groups showed no significant areas of differential activation.

The reverse contrast ((SH + SL) > (MH + ML)) showed regions where activation was greater when static visual stimuli were presented (Fig. 3). Again, there were no group differences when a direct contrast was performed. In the patients, activation was observed in the superior temporal gyri bilaterally, as well as in the left parietal operculum. In controls, similar activation was observed within the parietal and temporal lobes, with peaks of activation in the right planum temporale and parietal operculum, as well as within the supramarginal gyri bilaterally. In addition, significant activation for this contrast was seen in the midline and left cerebellum, with a peak of activity in the left VI region in the control group (Table 2).

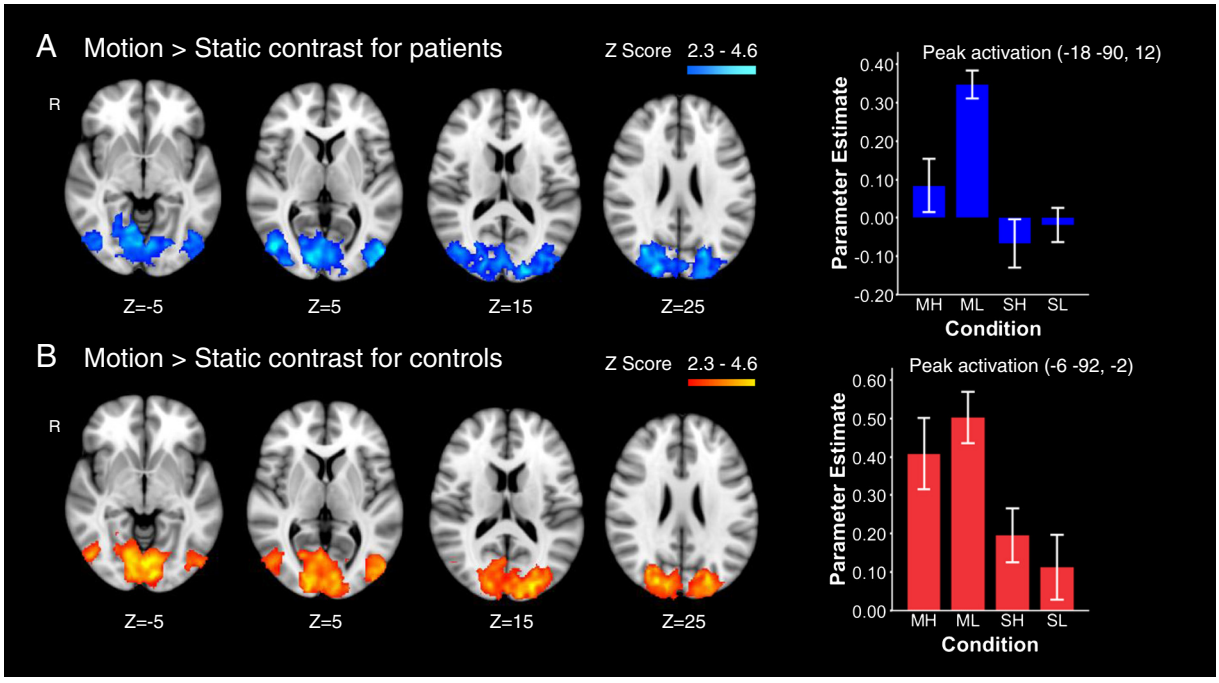

Fig. 2. The response to visual motion. Significant activation is shown for the contrast of moving versus static stimuli (MH + ML) > (SH + SL) in patients (A) and controls (B). Plots show the parameter estimates for the four conditions: visual motion/high proprioception (MH), visual motion/low proprioception (ML), static/high proprioception (SH), and static/low proprioception (SL), taken from a 10 mm diameter sphere centred in the activation cluster for the contrast for patients (MNI coordinates −18, −90, 12) and controls (−6, −92, −2). The results are superimposed on the MNI 152 T1 brain template. Right hemisphere is marked (R). Colour bar illustrates the Z score for the activation maps. Standard thresholding was used, with a height threshold of Z = 2.3 and a cluster threshold of $p < 0.05$.

3.2. Main effect of proprioception

Increased activation within the temporal lobes was observed for the main effect of High > Low proprioceptive input ((MH + SH) > (ML + SL)). In controls, high proprioceptive input was associated with increased activation in the left temporal lobe, with activation extending across the inferior and middle temporal gyri and the parahippocampal gyrus. In patients, the same contrast was associated with increased activation bilaterally in the temporal poles and parahippocampal gyri. There were no significant group differences in this contrast.

The reverse contrast, i.e. Low > High proprioceptive input, did show significant group differences. In the patients, the contrast ((ML + SL) > (MH + SH)), showed extensive areas where activity in medial and lateral occipital regions was reduced when proprioceptive input was high (Fig. 4A, blue/light blue). In controls, reduced activation with high proprioceptive input was seen in the right middle and inferior frontal gyri, anterior cingulate cortex, premotor and somatosensory areas, as well as middle and superior temporal gyri. However, there was no effect of proprioceptive input in the occipital regions. A direct comparison between patients and controls confirmed that the effect of high-levels of proprioceptive input on visual cortical responses was significantly greater in the patients compared to controls (Fig. 4A, yellow/red). The greater effect of proprioception in patients compared to controls was seen in midline occipital regions, including the intracalcarine cortex and occipital pole (Table 3). The differential effects of proprioception in the two groups can be seen in Fig. 4B, where high proprioceptive input (MH and SH plots) is associated with greater activation than low input (ML and SL plots) in the control group, but the reverse pattern is seen in the patient group.

Table 1
Activation Cluster Local Maxima: Main Effect of Visual Motion. Z statistic is followed by MNI coordinates of the maxima.

Local cluster maxima	Z	x	y	z
Controls				
Left occipital	5.26	−22	−90	16
	5.21	−2	−80	−4
	5.08	−6	−92	−2
Left occipital (near MT/V5)	4.12	−44	−80	6
Right occipital	4.84	14	−78	−2
Right occipital (near MT/V5)	4.61	46	−70	−2
	4.14	50	−72	−10
	3.54	48	−74	10
Patients				
Left occipital	4.96	−18	−90	12
Left occipital (near MT/V5)	4.94	−50	−78	4
Right occipital	5.31	20	−86	18
Right occipital (near MT/V5)	5.41	46	−76	4
	4.81	50	−76	8

3.3. Interactions between visual motion and proprioception

High levels of proprioceptive input were associated with a specific reduction in the response to visual motion in the BVL patients. In the patient group, the interaction ((ML + SH) > (MH + SL)) showed an asymmetric pattern of activation in the left lateral occipital pole and the inferior part of the left lateral occipital cortex, with differential activation seen within V5/MT and surrounding regions (Fig. 5, Table 4). In addition, activation associated with this contrast was observed in the cerebellar vermis and in both cerebellar hemispheres. In controls there were no significant areas of activation for this contrast seen within occipital regions.

Using a whole brain corrected threshold, the direct group contrast for the interaction (ML + SH) > (MH + SL) showed no significant differences. However, a more lenient uncorrected threshold of $p < 0.001$ did show left lateralized group differences in activation within the lateral occipital pole, the inferior part of the lateral occipital cortex and the inferior temporal gyrus. Plots of the parameter estimates for the interaction suggested that the result in patients was being driven by the effect of proprioception in the context of visual motion i.e. ML and MH

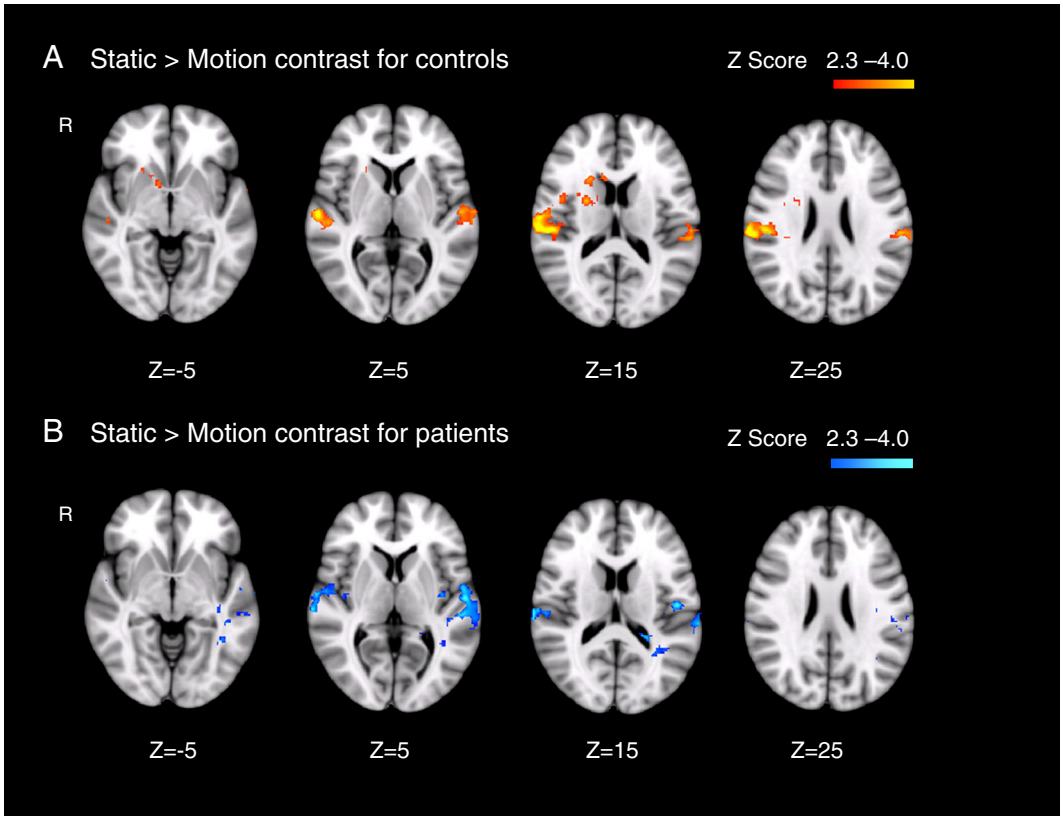

Fig. 3. The reverse contrast for visual motion ((SH + SL) > (MH + ML)) showing areas were activation is greater when static visual stimuli were presented. Thresholding is as in Fig. 2.

(Fig. 5B). This was confirmed by examining the results of the contrast of ML > MH. In the patients, this contrast showed activation in left lateral occipital areas, and activation was significantly higher in these regions for patients than controls using whole brain correction (Fig. 6, Table 5). Activation for ML > MH was also greater for the patients in the intracalcarine cortex bilaterally, the right occipital pole and the cerebellum. The other 'simple' contrasts from the interaction (i.e. ML vs. SL, SH vs. MH, and SH vs. SL) showed no significant group differences.

The reverse interaction ((MH + SL) > (ML + SH)) showed no significant activation for either patients or controls, and no significant difference between the groups.

Table 2
Activation Cluster Local Maxima: Reverse Effect of Visual Motion. Z statistic is followed by MNI coordinates of the maxima.

Local cluster maxima	Z	x	y	z
Controls				
Right planum temporale	4.05	60	−16	8
Right supramarginal gyrus	3.87	64	−24	24
Right parietal operculum	3.86	56	−24	16
Cerebellum, Left VI	3.49	−26	−58	−26
	3.30	−14	−68	−26
Cerebellum, Left I -IV	3.25	0	−54	−26
Left supramarginal gyrus	3.43	−62	−24	20
Left opercular	3.42	−54	−16	10
Patients				
Left superior temporal	3.94	−56	−10	0
	3.72	−52	−28	2
Left opercular	3.58	−54	−14	10
Right superior temporal	3.89	62	−22	12
	3.81	70	−22	8

3.4. Structural brain analysis

Voxel based morphometry analysis showed no significant differences in cortical structure between the patients with bilateral vestibular loss and the normal control subjects.

4. Discussion

There is already good evidence of interactions between vestibular and visual processing in humans from previous fMRI studies (Bense et al., 2001; Dieterich and Brandt, 2008; Dieterich et al., 2007). Here we demonstrate that proprioceptive and visual processing also interact in subjects with bilaterally reduced peripheral vestibular function (BVL patients). The reduction in visual motion-induced cortical activation in the presence of high proprioceptive stimulus suggests an inhibitory interaction between proprioceptive mediated head motion signals and visual cues. The findings suggest an upregulation of neck muscle proprioceptive signals as an adaptive response to bilateral loss of vestibular function. To our knowledge there is only one previous fMRI study assessing the effects of neck vibration with brain fMRI, although not in BVL patients (Fasold et al., 2008).

Our results are in keeping with recent work demonstrating that visual cortical regions have been shown to be a site of integration of visual and vestibular signals at the single cell level in animals. Neuronal recordings in Macaque monkeys show interactions between visual and vestibular input in multiple visual cortical areas, but not in vestibular areas such as the PIVC (Chen et al., 2008, 2010, 2011, 2012). Our result, a visuo-proprioceptive interaction, adds further evidence for integration of head motion/position signals occurring in visual processing areas.

In the presence of visual motion, proprioceptive input in the patient group had a lateralised effect on the visual cortex. The response to moving stimuli in regions including V5/MT and MST was reduced in BVL patients when proprioceptive input was high. Visual processing in

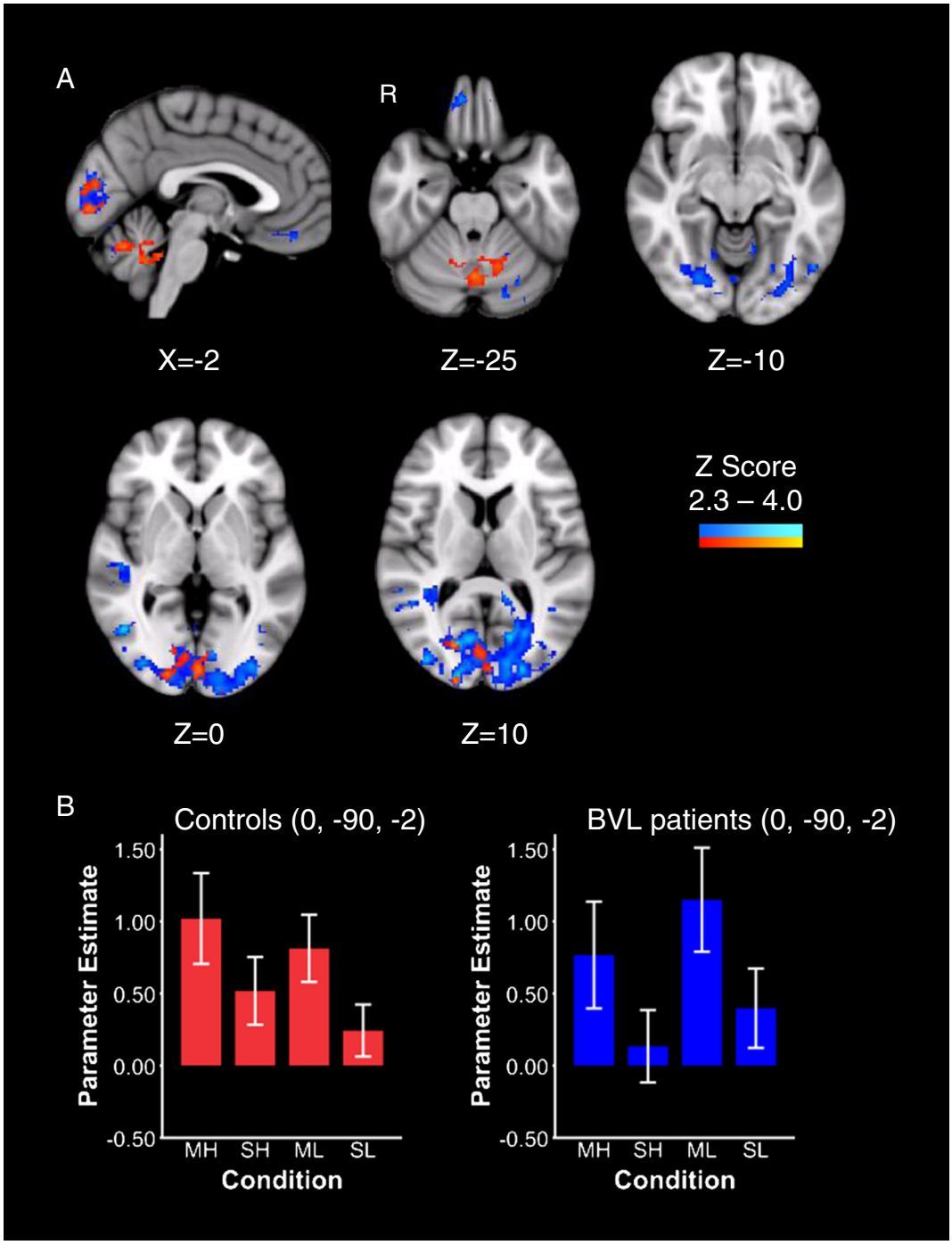

Fig. 4. Reduced response in visual cortex when proprioceptive input is high in BVL patients. (A) In patients, activity in the visual cortex is less when proprioceptive input is high relative to low ((ML + SL) > (MH + SH)) (blue/light blue regions). Superimposed on this result are regions where this difference was greater in the BVL group (red/yellow). These regions showed significantly less activation in the patients compared to controls for the main effect of High versus Low proprioceptive input ((MH + SH) > (ML + SL)). (B) Plots showing the parameter estimates for the four conditions in controls and patients, from the peak of the group difference in the visual cortex (MNI 0, −90, −2). Thresholding and presentation of results is as described in Fig. 2.

Table 3
Local maxima for activations in controls versus BVL patients for high versus low proprioceptive input.

Cluster local maxima	Z	x	y	z
Right intracalcarine	3.46	20	−76	12
Right occipital pole	3.32	22	−100	8
	3.27	32	−98	6
Midline occipital pole	3.12	0	−90	−2
Cerebellar vermis IX	3.28	0	−52	−36
Cerebellum vermis X	3.00	−2	−44	−32

these regions has been shown in previous studies to be sensitive to vestibular input (Bense et al., 2001), so the observed effects of high proprioceptive input in these areas is consistent with a 're-weighting' of sensory signals (Angelaki et al., 2009; Strupp et al., 1998).

The left hemispheric laterality we observed could be due to several factors. Given that all our subjects were right handed, and that both vestibular and visual motion fMRI effects are more prominent in the right hemisphere in right-handers (Bense et al., 2001; Dieterich and Brandt, 2008; Dieterich et al., 2003b), the more pronounced effects found in the left hemisphere cannot be explained solely on a handedness basis.

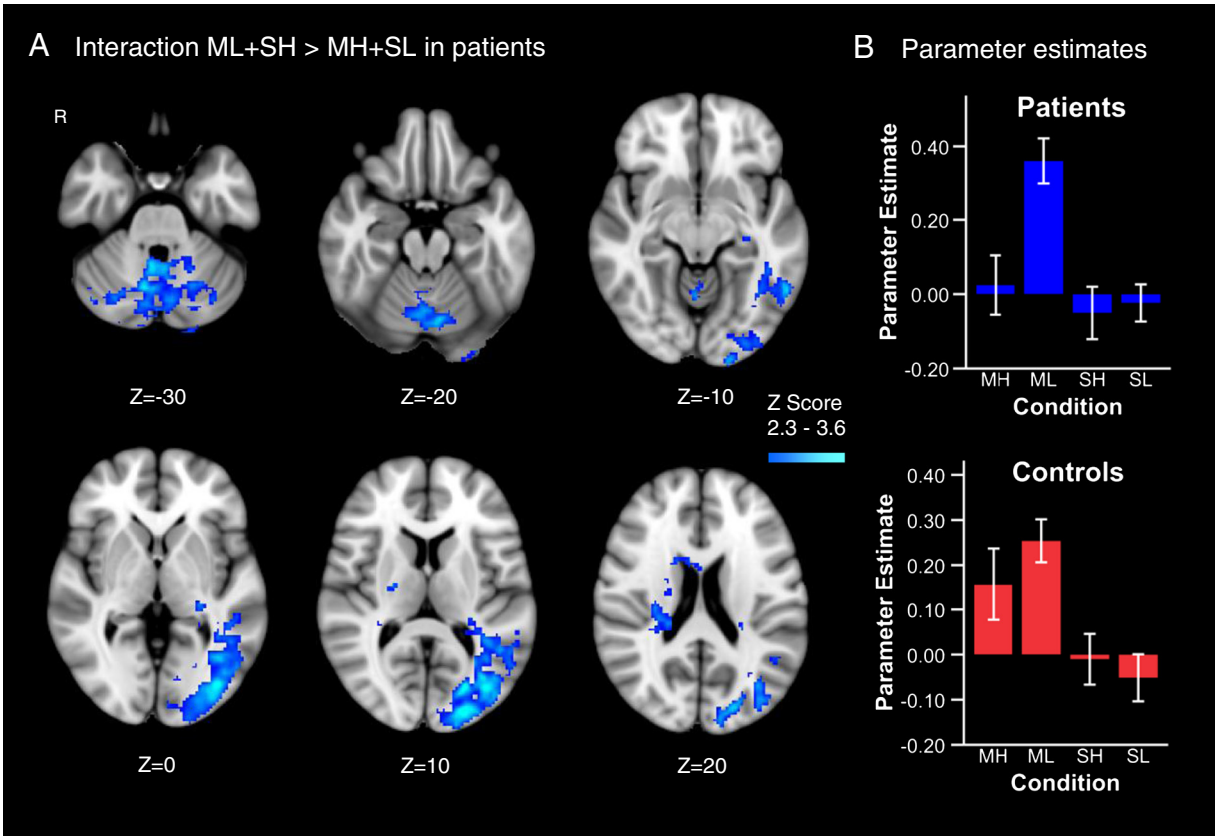

Fig. 5. Interaction between visual motion and proprioceptive input in BVL patients. (A) Brain regions showing a significant activation between visual motion and proprioceptive responses (ML + SH > MH + SL) in patients. (B) Plots of the parameter estimates for the four conditions in patients and, for the purpose of illustration, in controls using a 10 mm diameter sphere centred at the peak voxel of the interaction in patients (MNI coordinates −22, −92,10). Thresholding and presentation of results is as described in Fig. 2.

Alternatively, the stronger effects observed in the left hemisphere could be dictated by the characteristics of the stimuli employed. Both visual and proprioceptive stimuli were unilateral (left splenius vibration) or unidirectional (rightwards visual motion). Given that the signals from tendon and muscle vibration are interpreted as stretch of that muscle (Lekhel et al., 1997) a left splenius vibratory stimulus would be interpreted as if the head was turning to the right. The optokinetic stimulus to the right, in contrast, would signal that the head is turning to the left creating conflict between visual and proprioceptive signals mediating angular head motion input. It is well established that in such situations of sensory conflict, inertial receptors, in particular proprioceptive (Bronstein, 1986), are dominant ("have the final say") as they are less prone to ambiguity than visual mechanisms. For instance, visual motion to the right can be interpreted as object motion to the right or as head motion to the left; (Guerraz et al., 2001; Kleinschmidt et al., 2002). One would strongly suspect that resolving such directional conflict should elicit asymmetric activation of the cerebral hemispheres, as shown here, although predicting which hemisphere would be more activated is difficult. According to our findings, it seems that the hemisphere on the same side of the activated muscle is predominantly activated during the visuo-proprioceptive interaction, even though isolated proprioceptive effects were present in both hemispheres here and in the previous studies in normal subjects (Biguer et al., 1988; Fasold et al., 2008). Future experiments with separate right and left neck vibrations are necessary to fully prove this point. The fact that the patients have no vestibular function (which would further contribute

Table 4
Activation cluster local maxima for interaction of ML + SH > MH + SL in BVL patients.

Cluster local maxima	Z	x	y	z
Left lateral occipital pole	3.94	−22	−92	10
Left occipital (near V5/MT)	3.81	−36	−76	8
Left lateral occipital, inferior (near V5/MT)	3.7	−36	−86	2
Cerebellar vermis, right X	3.68	4	−50	−32
Cerebellar vermis, right VI	3.6	6	−70	−26
Cerebellum, left VI	3.67	−10	−72	−24
Cerebellum, crus, right I	3.62	36	−74	−34
Cerebellum, right VIIIb	3.53	10	−66	−30

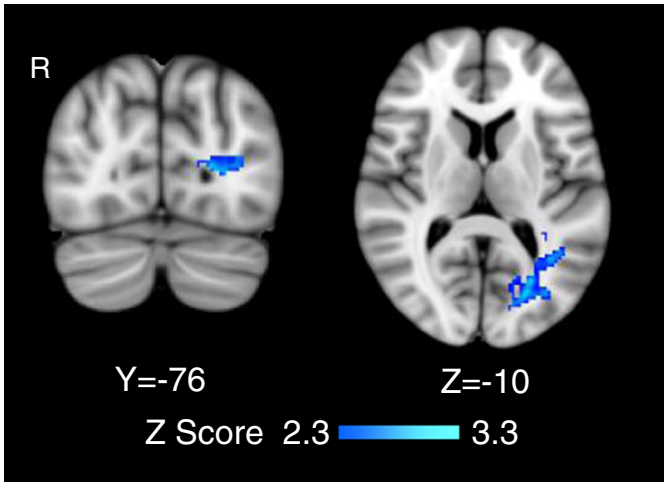

Fig. 6. Reduced response to visual motion stimulus in BVL patients. Brain regions showing more activation in patients than controls for the contrast of low vs. high proprioceptive input in the context of visual motion simulation (ML > MH). Thresholding and presentation of results is as described in Fig. 2.

Table 5
Activation cluster local maxima for ML > MH, patients > controls.

Cluster local maxima	Z	x	y	z
Left lateral occipital cortex	4.31	−18	−84	20
	4.02	−40	−82	18
	4.02	−22	−90	10
Left intracalcarine	4.08	−18	−64	8
Right occipital pole	4.10	20	−98	10
Cerebellar vermis, IX	3.90	0	−54	−32
Left cerebellum, crus I	3.96	−48	−54	−32
Left cerebellum VI	3.72	−26	−64	−30

to disambiguating the sensory conflict) also helps explain why the proprioceptive loop is upregulated in BVL patients.

The cerebellum has previously been shown to play a role in mediating enhancement of cervical proprioceptive responses in patients with diminished vestibular function (Bronstein et al., 1991). Similarly, the influence of vision on postural control (Guerraz and Day, 2005) and spatial orientation (Bisdorff et al., 1996) increases in patients with BVL. In agreement, only our BVL group showed an fMRI interaction between visual motion and neck vibration signals in the cerebellar vermis, where single unit recordings have shown proprioceptive, visual and vestibular interaction (Precht et al., 1976; Wilson et al., 1975a, 1975b). Whether the cerebellar fMRI signal identified reflects changes in a local subcortical network, or is a marker or 'relay station' reflecting cortical changes (Meng et al., 2007), or both, cannot be ascertained at present.

The factorial design applied allows us to control for some potential confounding factors. The interaction is unlikely be an artifact of physical movement generated by the vibrating stimulator, as the effect on V5/MT and other lateral occipital regions was dependent on visual input, i.e. the same vibratory input only reduced visual cortical activation in the presence of visual motion.

Eye movements could be a potential confounder, however the factorial design means that observed differences are driven by the stimuli. Furthermore, the pattern of eye movement elicited by the visual and cervical proprioceptive stimuli used here is identical in both subject groups — essentially optokinetic nystagmus unaffected by neck vibration. The recent observation that MRI scanner magnetic fields can induce vestibular effects (Roberts et al., 2011) cannot explain our results either given that the magnetic field was constant across all four conditions, or could not produce the interaction we observed between visual motion and proprioception.

The difference in physiological response we have demonstrated was not the result of gross differences in brain anatomy. Our VBM study showed no significant differences between the patient and control groups. Previous reports have shown structural changes due to vestibular neuritis and acoustic neuroma surgery (Helmchen et al., 2011; zu Eulenburg et al., 2010), but these are unilateral conditions producing highly asymmetric ascending vestibular signals. In contrast to our normal structural results, one study in 10 subjects with BVL due to Neurofibromatosis type 2 reported hippocampal atrophy (Brandt et al., 2005). Although we cannot provide an unequivocal explanation for this discrepancy, the fact that the vestibular loss was due to bilateral vestibular schwannoma with significant degrees of hearing loss and other potential effects from the underlying Neurofibromatosis type 2, may partly explain the difference between the two studies.

Our approach to delivering proprioceptive stimulation in the scanner was novel. A custom Dacron and Nylon vibrating device powered by the medical air supply was developed for this experiment. The absence of any electromagnetic materials ensures this is safe and does not produce signal artifact on MRI acquisition. Our device produced a greater displacement 0.4 mm, in comparison to 0.2 mm for a piezo-ceramic device reported by Fasold et al. (2008). The piezo-ceramic device has an advantage of being able to be precisely tuned to desired frequencies 'on-line'; our device has a limited range of frequencies available 'on-line', although as shown, can produce frequencies appropriate for proprioceptive stimuli.

5. Conclusion

Neck proprioceptive and visual motion signals interact, and this effect differs between normal subjects and patients with acquired bilateral vestibular loss. This visuo-proprioceptive interaction found in BVL subjects resembles the visuo-vestibular interaction described in fMRI studies, both during vestibular activation and vertigo, lending support to the notion that neck proprioceptive input partly takes over vestibular functions in BVL patients. The overlap of visual motion, proprioceptive and vestibular cortical areas identified in humans and other primates supports 'polysensory' cortical networks responsible for spatial orientation, balance, self motion perception where these signals interact. Clinically, the findings support a prominent role for cervico-proprioceptive inputs in the process of recovery and compensation in patients with bilateral vestibular failure.

Conflicts of interest

The authors have no conflicts of interest to declare.

Funding

NJC was employed at Imperial College with a MRC programme grant (held by AMB); and is currently employed by the Southern District Health Board and the University of Otago, Dunedin, New Zealand.

DJS is employed at Imperial College, funded by the National Institute of Health Research (UK) and the Imperial College Healthcare Charity.

GPS is employed at Imperial College on a GSK-Wellcome PhD Fellowship.

ADW is employed in the Department of Imaging, Imperial College NHS trust.

AMB is employed at Imperial College, Neuro-otology, Division of Brain Sciences and is funded by the Medical Research Council (UK).

Acknowledgements

Technical MRI assistance for this project was provided by Anastasia Papadaki, Physicist, Radiological Sciences Unit, Imperial College.

The vibrotactile device fabrication and C/C++ coding was assisted by Dave Buckwell, Neuro-otology, Imperial College, London.

Eye movement recordings were done by Dr Ed Roberts, Post Doctoral Research Fellow, Neuro-otology, Imperial College, London.

References

Akbarian, S., Grusser, O.J., Guldin, W.O., 1992. Thalamic connections of the vestibular cortical fields in the squirrel monkey (Saimiri sciureus). J. Comp. Neurol. 326 (3), 423–441 (Dec 15).

Angelaki, D.E., Gu, Y., DeAngelis, G.C., 2009. Multisensory integration: psychophysics, neurophysiology, and computation. Curr. Opin. Neurobiol. 19 (4), 452–458 (Aug).

Ashburner, J., Friston, K.J., 2000. Voxel-based morphometry — the methods. NeuroImage 11 (6 Pt 1), 805–821 (Jun).

Beckmann, C.F., Jenkinson, M., Smith, S.M., 2003. General multilevel linear modeling for group analysis in FMRI. NeuroImage 20 (2), 1052–1063 (Oct).

Bense, S., Stephan, T., Yousry, T.A., Brandt, T., Dieterich, M., 2001. Multisensory cortical signal increases and decreases during vestibular galvanic stimulation (fMRI). J. Neurophysiol. 85 (2), 886–899 (Feb).

Biguer, B., Donaldson, I.M., Hein, A., Jeannerod, M., 1988. Neck muscle vibration modifies the representation of visual motion and direction in man. Brain 111 (Pt 6), 1405–1424 (Dec).

Bisdorff, A.R., Wolsley, C.J., Anastasopoulos, D., Bronstein, A.M., Gresty, M.A., 1996. The perception of body verticality (subjective postural vertical) in peripheral and central vestibular disorders. Brain 119 (Pt 5), 1523–1534 (Oct).

Bottini, G., Karnath, H.O., Vallar, G., Sterzi, R., Frith, C.D., Frackowiak, R.S., et al., 2001. Cerebral representations for egocentric space: functional–anatomical evidence from caloric vestibular stimulation and neck vibration. Brain 124 (Pt 6), 1182–1196 (Jun).

Bove, M., Courtine, G., Schieppati, M., 2002. Neck muscle vibration and spatial orientation during stepping in place in humans. J. Neurophysiol. 88 (5), 2232–2241 (Nov).

Brandt, T., Bartenstein, P., Janek, A., Dieterich, M., 1998. Reciprocal inhibitory visual–vestibular interaction. Visual motion stimulation deactivates the parieto-insular vestibular cortex. Brain 121 (Pt 9), 1749–1758 (Sep).
Brandt, T., Schautzer, F., Hamilton, D.A., Bruning, R., Markowitsch, H.J., Kalla, R., et al., 2005. Vestibular loss causes hippocampal atrophy and impaired spatial memory in humans. Brain 128 (Pt 11), 2732–2741 (Nov).
Bronstein, A.M., 1986. Suppression of visually evoked postural responses. Exp. Brain Res. 63 (3), 655–658.
Bronstein, A.M., Hood, J.D., 1986. The cervico-ocular reflex in normal subjects and patients with absent vestibular function. Brain Res. 373 (1–2), 399–408 (May 14).
Bronstein, A.M., Hood, J.D., 1987. Oscillopsia of peripheral vestibular origin. Central and cervical compensatory mechanisms. Acta Otolaryngol. 104 (3–4), 307–314 (Sep-Oct).
Bronstein, A.M., Mossman, S., Luxon, L.M., 1991. The neck-eye reflex in patients with reduced vestibular and optokinetic function. Brain 114 (Pt 1A), 1–11 (Feb).
Chen, A., Gu, Y., Takahashi, K., Angelaki, D.E., Deangelis, G.C., 2008. Clustering of self-motion selectivity and visual response properties in macaque area MSTd. J. Neurophysiol. 100 (5), 2669–2683 (Nov).
Chen, A., DeAngelis, G.C., Angelaki, D.E., 2010. Macaque parieto-insular vestibular cortex: responses to self-motion and optic flow. J. Neurosci. 30 (8), 3022–3042 (Feb 24).
Chen, A., DeAngelis, G.C., Angelaki, D.E., 2011. Representation of vestibular and visual cues to self-motion in ventral intraparietal cortex. J. Neurosci. 31 (33), 12036–12052 (Aug 17).
Chen, A., DeAngelis, G.C., Angelaki, D.E., 2012. Convergence of vestibular and visual self-motion signals in an area of the posterior sylvian fissure. J. Neurosci. 31 (32), 11617–11627 (Aug 10).
Cousins, S., Kaski, D., Cutfield, N., Seemungal, B., Golding, J.F., Gresty, M., et al., 2013. Vestibular perception following acute unilateral vestibular lesions. PLoS One 8 (5), e61862.
Deutschlander, A., Hufner, K., Kalla, R., Stephan, T., Dera, T., Glasauer, S., et al., 2008. Unilateral vestibular failure suppresses cortical visual motion processing. Brain 131 (Pt 4), 1025–1034 (Apr).
Dichgans, J., Bizzi, E., Morasso, P., Tagliasco, V., 1973. Mechanisms underlying recovery of eye-head coordination following bilateral labyrinthectomy in monkeys. Exp. Brain Res. 18 (5), 548–562 (Dec 20).
Dieterich, M., Brandt, T., 2008. Functional brain imaging of peripheral and central vestibular disorders. Brain 131 (Pt 10), 2538–2552 (Oct).
Dieterich, M., Bense, S., Stephan, T., Yousry, T.A., Brandt, T., 2003a. fMRI signal increases and decreases in cortical areas during small-field optokinetic stimulation and central fixation. Exp. Brain Res. 148 (1), 117–127 (Jan).
Dieterich, M., Bense, S., Lutz, S., Drzezga, A., Stephan, T., Bartenstein, P., et al., 2003b. Dominance for vestibular cortical function in the non-dominant hemisphere. Cereb. Cortex 13 (9), 994–1007 (Sep).
Dieterich, M., Bauermann, T., Best, C., Stoeter, P., Schlindwein, P., 2007. Evidence for cortical visual substitution of chronic bilateral vestibular failure (an fMRI study). Brain 130 (Pt 8), 2108–2116 (Aug).
Elhawary, H., Zivanovic, A., Tse, Z.T., Rea, M., Davies, B.L., Young, I., et al., 2008. A magnetic-resonance-compatible limb-positioning device to facilitate magic angle experiments *in vivo*. Proc. Inst. Mech. Eng. H 222 (5), 751–760 (Jul).
Fasold, O., Heinau, J., Trenner, M.U., Villringer, A., Wenzel, R., 2008. Proprioceptive head posture-related processing in human polysensory cortical areas. Neuroimage 40 (3), 1232–1242 (Apr 15).
Gdowski, G.T., Belton, T., McCrea, R.A., 2001. The neurophysiological substrate for the cervico-ocular reflex in the squirrel monkey. Exp. Brain Res. 140 (3), 253–264 (Oct).
Good, C.D., Johnsrude, I.S., Ashburner, J., Henson, R.N., Friston, K.J., Frackowiak, R.S., 2001. A voxel-based morphometric study of ageing in 465 normal adult human brains. NeuroImage 14 (1 Pt 1), 21–36 (Jul).
Gresty, M.A., Hess, K., Leech, J., 1977. Disorders of the vestibulo-ocular reflex producing oscillopsia and mechanisms compensating for loss of labyrinthine function. Brain 100 (4), 693–716 (Dec).
Guerraz, M., Day, B.L., 2005. Expectation and the vestibular control of balance. J. Cogn. Neurosci. 17 (3), 463–469 (Mar).
Guerraz, M., Thilo, K.V., Bronstein, A.M., Gresty, M.A., 2001. Influence of action and expectation on visual control of posture. Brain Res. Cogn. Brain Res. 11 (2), 259–266 (Apr).
Guldin, W.O., Akbarian, S., Grusser, O.J., 1992. Cortico-cortical connections and cytoarchitectonics of the primate vestibular cortex: a study in squirrel monkeys (Saimiri sciureus). J. Comp. Neurol. 326 (3), 375–401 (Dec 15).
Helmchen, C., Klinkenstein, J.C., Kruger, A., Gliemroth, J., Mohr, C., Sander, T., 2011. Structural brain changes following peripheral vestibulo-cochlear lesion may indicate multisensory compensation. J. Neurol. Neurosurg. Psychiatry 82 (3), 309–316 (Mar).
Jenkinson, M., Smith, S., 2001. A global optimisation method for robust affine registration of brain images. Med. Image Anal. 5 (2), 143–156 (Jun).
Kammerlind, A.S., Ledin, T.E., Skargren, E.I., Odkvist, L.M., 2005. Long-term follow-up after acute unilateral vestibular loss and comparison between subjects with and without remaining symptoms. Acta Otolaryngol. 125 (9), 946–953 (Sep).
Karlberg, M., Aw, S.T., Black, R.A., Todd, M.J., MacDougall, H.G., Halmagyi, G.M., 2003. Vibration-induced ocular torsion and nystagmus after unilateral vestibular deafferentation. Brain 126 (Pt 4), 956–964 (Apr).
Kasai, T., Zee, D.S., 1978. Eye-head coordination in labyrinthine-defective human beings. Brain Res. 144 (1), 123–141 (Apr 7).
Kleinschmidt, A., Thilo, K.V., Buchel, C., Gresty, M.A., Bronstein, A.M., Frackowiak, R.S., 2002. Neural correlates of visual-motion perception as object- or self-motion. Neuroimage 16 (4), 873–882 (Aug).
Lekhel, H., Popov, K., Anastasopoulos, D., Bronstein, A., Bhatia, K., Marsden, C.D., et al., 1997. Postural responses to vibration of neck muscles in patients with idiopathic torticollis. Brain 120 (Pt 4), 583–591 (Apr).
Magnus, R., De Kleijn, A., 1912. Die Abhangigkeit des Tonus der Extremitatenmuskeln von der Kopfstellung. Pflugers Arch. 145, 455–548.
Malikovic, A., Amunts, K., Schleicher, A., Mohlberg, H., Eickhoff, S.B., Wilms, M., et al., 2007. Cytoarchitectonic analysis of the human extrastriate cortex in the region of V5/MT+: a probabilistic, stereotaxic map of area hOc5. Cereb. Cortex 17 (3), 562–574 (Mar).
Meng, H., May, P.J., Dickman, J.D., Angelaki, D.E., 2007. Vestibular signals in primate thalamus: properties and origins. J. Neurosci. 27 (50), 13590–13602 (Dec 12).
Popov, K., Lekhel, H., Bronstein, A., Gresty, M., 1996. Postural responses to vibration of neck muscles in patients with unilateral vestibular lesions. Neurosci. Lett. 214 (2–3), 202–204 (Aug 23).
Popov, K.E., Lekhel, H., Faldon, M., Bronstein, A.M., Gresty, M.A., 1999. Visual and oculomotor responses induced by neck vibration in normal subjects and labyrinthine-defective patients. Exp. Brain Res. 128 (3), 343–352 (Oct).
Precht, W., Simpson, J.I., Llinas, R., 1976. Responses of Purkinje cells in rabbit nodulus and uvula to natural vestibular and visual stimuli. Pflugers Arch. 367 (1), 1–6 (Nov 30).
Rinne, T., Bronstein, A.M., Rudge, P., Gresty, M.A., Luxon, L.M., 1998. Bilateral loss of vestibular function: clinical findings in 53 patients. J. Neurol. 245 (6–7), 314–321 (Jun-Jul).
Roberts, D.C., Marcelli, V., Gillen, J.S., Carey, J.P., Della Santina, C.C., Zee, D.S., 2011. MRI magnetic field stimulates rotational sensors of the brain. Curr. Biol. 21 (19), 1635–1640 (Oct 11).
Sadeghi, S.G., Minor, L.B., Cullen, K.E., 2011. Multimodal integration after unilateral labyrinthine lesion: single vestibular nuclei neuron responses and implications for postural compensation. J. Neurophysiol. 105 (2), 661–673 (Feb).
Smith, S.M., 2002. Fast robust automated brain extraction. Hum. Brain Mapp. 17 (3), 143–155 (Nov).
Smith, S.M., Jenkinson, M., Woolrich, M.W., Beckmann, C.F., Behrens, T.E., Johansen-Berg, H., et al., 2004. Advances in functional and structural MR image analysis and implementation as FSL. NeuroImage 23 (Suppl. 1), S208–S219.
Strupp, M., Arbusow, V., Dieterich, M., Sautier, W., Brandt, T., 1998. Perceptual and oculomotor effects of neck muscle vibration in vestibular neuritis. Ipsilateral somatosensory substitution of vestibular function. Brain 121 (Pt 4), 677–685 (Apr).
Wilson, V.J., Maeda, M., Franck, J.I., 1975a. Input from neck afferents to the cat flocculus. Brain Res. 89 (1), 133–138 (May 16).
Wilson, V.J., Maeda, M., Franck, J.I., 1975b. Inhibitory interaction between labyrinthine, visual and neck inputs to the cat flocculus. Brain Res. 96 (2), 357–360 (Oct 17).
Wuyts, F.L., Hoppenbrouwers, M., Pauwels, G., Van de Heyning, P.H., 2003. Utricular sensitivity and preponderance assessed by the unilateral centrifugation test. J. Vestib. Res. 13 (4–6), 227–234.
Xerri, C., Gianni, S., Manzoni, D., Pompeiano, O., 1985. Central compensation of vestibular deficits. IV. Responses of lateral vestibular neurons to neck rotation after labyrinth deafferentation. J. Neurophysiol. 54 (4), 1006–1025 (Oct).
Zhang, Y., Brady, M., Smith, S., 2001. Segmentation of brain MR images through a hidden Markov random field model and the expectation-maximization algorithm. IEEE Trans. Med. Imaging 20 (1), 45–57 (Jan).
Zingler, V.C., Weintz, E., Jahn, K., Mike, A., Huppert, D., Rettinger, N., et al., 2008. Follow-up of vestibular function in bilateral vestibulopathy. J. Neurol. Neurosurg. Psychiatry 79 (3), 284–288 (Mar).
zu Eulenburg, P., Stoeter, P., Dieterich, M., 2010. Voxel-based morphometry depicts central compensation after vestibular neuritis. Ann. Neurol. 68 (2), 241–249 (Aug).